One- and three-dimensional photoconductive response of highly oriented polyacetylene

R. Tubino, R. Dorsinville, A. Seas, J. Birman, and R. R. Alfano
Institute for Ultrafast Spectroscopy and Lasers, Electrical Engineering and Physics Departments, The City College of the City University of New York, New York, New York 10031
(Received 25 March 1987; revised manuscript received 2 February 1988)

The *I-V* characteristic curve for the photocurrent flowing both parallel and perpendicular to the chain axis has been measured for a highly oriented form of *trans*-polyacetylene. The experimental data provide information on the influence of dimensionality on the charge transport. Onsager's dissociation theory accounts well, at least semiquantitatively, for the observed quantum efficiency for carrier generation as a function of the applied electric field, photon flux and energy, and temperature.

INTRODUCTION

The anisotropy of the optical, vibrational, and transport properties of polyacetylene can only be studied in samples possessing a high degree of orientational order. Polyacetylene synthesized, according to the procedure indicated by Shirakawa and co-workers,[1] consists of 20-nm fibrils which are randomly oriented. Within the fibrils the individual polyenic chains are arranged in a three-dimensional lattice of high regularity. The lack of preferential orientation of the fibers makes polyacetylene an essentially isotropic material. Recently, two synthetic routes to obtain a fully oriented material have been reported. One method proceeds via the preparation of a stretchable prepolymer,[2] which yields polyacetylene by pyrolysis. The other method, which adopts the Ziegler-Natta polymerization procedure, uses a Ti-based catalyst[3] to yield films of *cis*-polyacetylene 20–40 μm thick, which can be stretched up to seven times their original length. Highly oriented *trans*-polyacetylene (HOTPA) can be obtained by thermal isomerization of the pristine polymer. The material studied in our work has been prepared following the second route and is characterized by a relatively large density (1.0–1.1 g/cm^3) compared to that of polyacetylene prepared according to the Shirakawa method (0.4–0.5 g/cm^3).[3] The value of the density approaches the theoretical[4] crystallographic (1.15 g/cm^3). X-ray diffraction patterns of similarly prepared samples have shown a very high level of preferred orientation of the crystallites with the chain axis parallel to the stretching direction.[3]

HOTPA shows a strong anisotropy of its optical properties. An accurate interference study using infrared radiation has revealed[4] strong anisotropy of the refractive index ($n_\perp/n_\parallel=1.9$) and dielectric constant. All the infrared absorption bands exhibit clear polarization properties in agreement with group selection rules.[5] Additional information on the microscopic structure of the polymer have been obtained using resonant Raman scattering.[6,7] The intensity ratios for the various scattering configurations have indicated the presence of segments with short conjugation lengths. This shows the existence of various defects (chain termination, cross link, oxidation, deviation from planarity, etc.) responsible for the interruption of the conjugation path. The relative content of short chains in the polymer material increases as the sample deteriorates following its exposure to oxygen.

The anisotropic character of the charge transport in conjugated polymers arises from the large difference between intra and interchain overlap integrals. The large overlap between atomic wave functions along the chain gives rise to the formation of strong π covalent bonds, while the small overlap between adjacent chains is responsible for the weak van der Waals bonding. In polyacetylene, charge carriers can be created by doping or photogeneration. The interpretation of the conductivity data of chemically doped samples is complicated by the fact that the excess charge carriers created by the charge transfer are bound to the dopant counterion. Since doping inevitably increases the disorder and reduces the average length of the conjugation path, no information on the charge motion in the pristine polymer can be readily inferred using doped samples, whose electrical transport properties are essentially controlled by hopping processes. Steady-state[8–12] and pulsed photoconductivity[13,14] of unoriented Shirakawa polyacetylene films have been studied by several groups. Recently we have studied the anisotropy of the photoinduced absorption and the photoconductivity in HOTPA.[15] Photoconductivity measurements have also been carried out on polyacetylene obtained from a stretched prepolymer[16] showing an anisotropic behavior for an applied external electric field parallel and perpendicular to the chain direction as well as for different polarization angles of the incident light.

The goal of this paper is to present and discuss the anisotropic behavior of the motion of the photogenerated charge carriers in HOTPA using photoconductivity measurements. In order to gain a better understanding of the carrier photogeneration and their subsequent transport in the polymer lattice in response to an applied external field, we have investigated the photoresponse of HOTPA as a function of the applied electric field E, of the temperature T, and of the direction of the current flow with respect to the stretching direction. These measurements show that, as in the case of single crystals of polydiace-

tylene,[17,18] HOTPA appears to be capable of exhibiting either one- or three-dimensional behavior of the motion of the charge carriers depending on the direction of the current flow with respect to the carbon skeleton of the polymer. We will first present the experimental results and then we will discuss a model for the kinetics of the oppositely charged carrier separation, which accounts for the various experimental features observed.

METHOD

The photoexcitation was achieved by a cw argon-ion laser. Copper electrodes were connected by pressure to 2×5 mm free-standing 50-μm-thick stretched polyacetylene films and the current-voltage characteristic was measured with the electrodes placed along the stretching direction (1D or $\parallel$ case) or perpendicular to that direction (3D or $\perp$ case). The spacing between the electrodes was about 0.36 mm in all the experiments. The total incident light power on the sample varied between 0.4 and 15 mW. The photocurrent was determined in two steps. First the dark current was measured, then the sample was uniformly illuminated with the laser beam. The photocurrent was obtained by subtracting the dark current from the total current measured. The *I-V* dependence of the dark current in the 3D case is shown in Fig. 1. The *I-V* characteristic is linear and symmetrical for positive and negative voltages over the range of field values used in the experiments showing the conductive response expected in a sample with Ohmic contacts. The conductivity was evaluated in both 1D and 3D cases and found to be in the 10^{-6}–10^{-7} $(\Omega\,\mathrm{cm})^{-1}$ range. These values are in good agreement with previously published data[19] for unoriented *trans*-polyacetylene samples and support the assumption that the pressure contacts used in this experiment are nonblocking, low-resistivity contacts. For the temperature measurements, cold nitrogen gas was blown on the samples inside a nitrogen Dewar. Thermocouples were used to monitor the temperature.

RESULTS

Figures 2–4 show the dependence of the photocurrent on the electric field for a sample of stretched *trans*-polyacetylene for the two cases of current flowing along and perpendicular to the stretching direction for different laser intensities at 514 nm. Figure 5 shows the *I-V* characteristic at three different wavelengths 488, 514, and 458 nm. These figures show a number of interesting features.

(i) The photocurrent ratio along the stretching direction relative to that perpendicular to the stretching direction is about 10 (Figs. 2 and 3), in agreement with conductivity data from chemically doped samples. This value indicates, as expected, that the initially excited carriers move more easily along the chain than in the perpendicular direction.

(ii) A comparison of the curves for 488 and 514 nm (Fig. 5) shows that the photocurrent intensity increases with the photon energy even well above the gap, as ob-

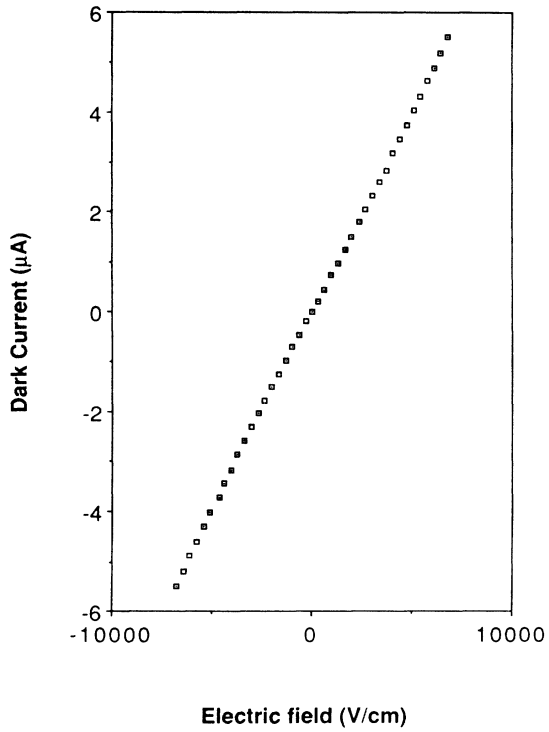

FIG. 1. Dependence of the dark current on electric field in the 3D ($\perp$) case.

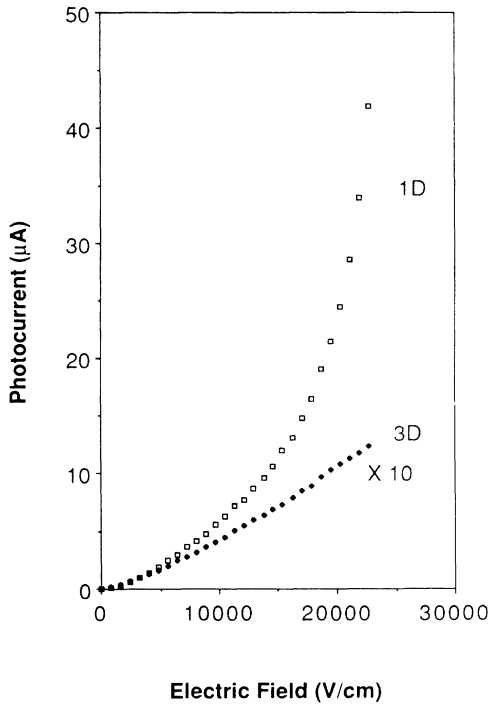

FIG. 2. Photocurrent as a function of the electric field E in the 3D ($\perp$) and 1D ($\parallel$) cases at 4 mW excitation power and $\lambda=514$ nm.

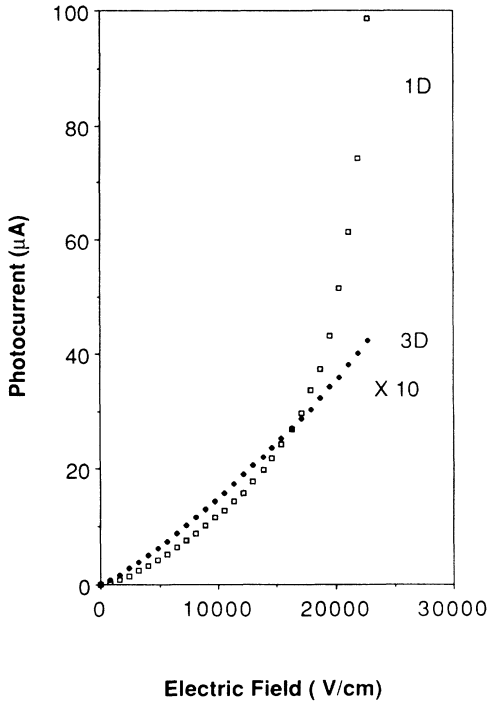

FIG. 3. Photocurrent as a function of the electric field E in the 3D ($\perp$) and 1D ($\parallel$) cases at 15 mW excitation power and $\lambda = 514$ nm.

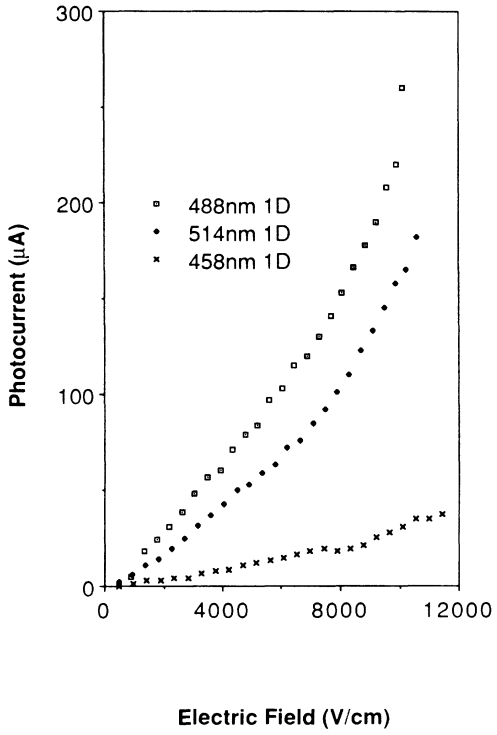

FIG. 5. Photocurrent as a function of the electric field E in the 1D ($\parallel$) case at 8 mW excitation power and $\lambda = 458$ ($\times$), 488 ($\boxdot$), and 514 nm ($\blacklozenge$).

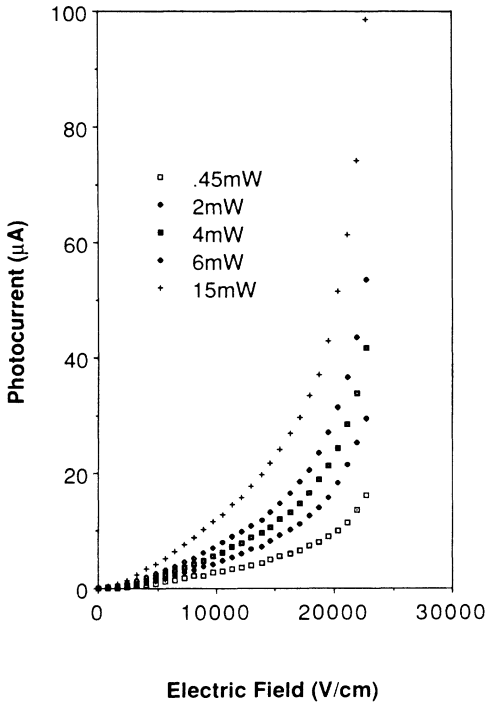

FIG. 4. Photocurrent as a function of the electric field E in the 1D ($\parallel$) case at increasing excitation power from 0.45 to 15 mW and $\lambda = 514$ nm.

served in unoriented samples.[11] Figure 5 shows the effect of the sample deterioration, due to exposure to oxygen, on the photoresponse of stretched *trans*-polyacetylene films. The data obtained with 458 nm refer to a sample which has been exposed to oxygen for several days. In this case, the photocurrent is weaker and the photoconductivity anisotropy (not shown in Fig. 5) is greatly reduced and the nonlinear behavior of the parallel photocurrent is no longer observed.

(iii) The field dependence of the photocurrent for the two directions, parallel and perpendicular to a line drawn between the two electrodes, clearly changes with the direction of the charge transport. For a perpendicular orientation corresponding to a current flow perpendicular to the stretching direction, the behavior of the photocurrent is linear becoming slightly superlinear at relatively high fields ($> 10\,000$ V/cm). On the contrary, in the parallel case corresponding to a current flow along the chains, the dependence of the photocurrent on the electric field is clearly nonlinear. This behavior is illustrated in Figs. 2 and 3, where the photocurrent is plotted as a function of the electric field for two laser intensities 4 and 15 mW, respectively. Figure 4 shows that the nonlinear behavior in the parallel case is present at intensities as low as 0.45 mW and as high as 15 mW. We have carried out photocurrent measurements for different wavelengths (514, 488, and 458 nm) and intensities (between 0.4 and 15 mW), and the character of both parallel and perpendicular curves did not substantially change.

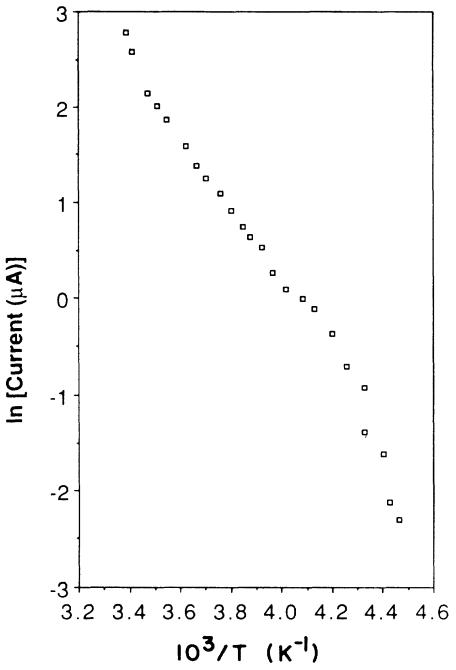

FIG. 6. Temperature dependence of the 1D (||) current in HOTPA. The excitation wavelength was 514 nm.

Figures 6 and 7 show the temperature dependence of the parallel and perpendicular currents. It is clear that in both cases the steady-state current decreases rapidly with the temperature and no appreciable photocurrent is detected below 200 K. This behavior is quite different from the transient photoconductivity case which is essentially temperature independent.[14]

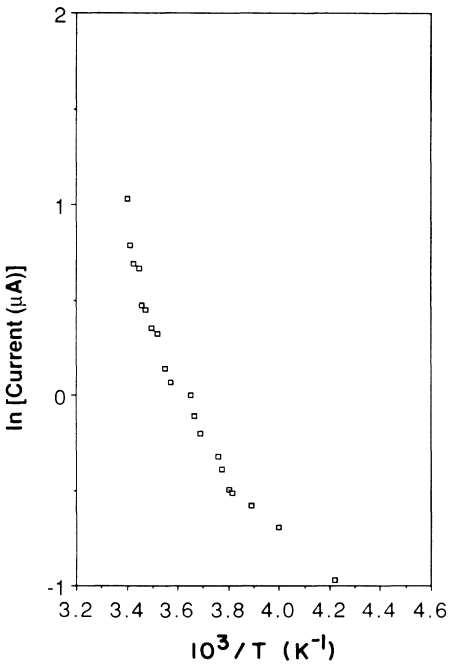

FIG. 7. Temperature dependence of the 3D (⊥) current in HOTPA. The excitation wavelength was 514 nm.

DISCUSSION

It is now widely accepted that in polyacetylene the nature of the charge carriers (both photogenerated or created by doping) is quite different from conventional 3D semiconductors.[20] The strong electron-phonon interaction together with the 1D character of the polymeric structure plays a significant role in determining the self-localization of the photogenerated carriers into soliton and polaron states.[21] Evidence for that is well established and comes mainly from magnetic as well as optical properties of polyacetylene. In fact, the main features observed in the photoinduced absorption spectrum of *trans*-polyacetylene (ir and near-ir region) are currently being interpreted as a signature of the lattice distortion around the soliton, which causes a perturbation in both vibrational and electronic states of the polyenic chain. However, because of their topological nature solitons can only exist in pairs and therefore, as has been discussed by Orenstein *et al.*,[20] when an excess electron is transferred to a nearby chain it forms a one-dimensional polaron, rather than a soliton. When a photon exceeding the energy gap is absorbed, an electron-hole pair is created, which is rapidly converted into a pair of oppositely charged solitons. Since the transition moment of the band-to-band transition is aligned with the chain direction, most of the soliton-antisoliton pairs are created in the same chain. The photoconductive response is expected to be dependent on the free carrier lifetime, the mobility and the probability to escape geminate recombination. The last two parameters should depend on the dimensionality of the carrier motion. In the following, we will show that the difference in the I-V characteristics for the 1D (||) and 3D (⊥) transport cases can be accounted for, at least qualitatively, by taking into account the dependence of the escape probability on the dimensionality.

To account for the dependence of the escape probability on the direction of the applied electric field with respect to the chain direction, we will use a model developed originally by Onsager[22] for electrolytic solutions, which studies the motion of oppositely charged carriers diffusing under the influence of an externally applied field. The obvious limitation of this model in the polyacetylene case is that it does not consider the coupling of the excess charge carriers with the lattice. However, the anisotropic version of Onsager's analysis has been proven effective in explaining the electric field, laser wavelength, and intensity dependence of the intrinsic photocurrent in polydiacetylenes,[17] which are quasi-one-dimensional organic systems with similar properties. This suggests that the model could be used for a qualitative understanding of the photocurrent characteristics in polyacetylene.

Following Onsager's model, the probability that an absorbed photon creates a pair of free oppositely charged carriers is given by $\eta\Phi$, where η is the probability of creation of a pair of hot carriers and Φ is the probability of escaping geminate recombination. For interband excitations, almost every absorbed photon creates a pair of thermalized carriers (thermalization distance a) bound by their mutual Coulomb attraction ($\eta = 1$).

In the 3D case, assuming isotropic motion of the car-

riers in the lattice, the probability of escaping geminate recombination as a function of the electric field for a pair of carriers with a separation a is given by the following series:[22]

$$\Phi_{3D}=e^{-r_c/a}\left[1+\frac{e}{kT}\frac{1}{2!}r_cE+\left[\frac{e}{kT}\right]^2\frac{1}{3!}r_c(\tfrac{1}{2}r_c-a)E^2+\left[\frac{e}{kT}\right]^3\frac{1}{4!}r_c(a^2-ar_c+\tfrac{1}{6}r_c^2)E^3+\cdots\right], \quad (1)$$

where $r_c=e^2/4\pi\epsilon kT$ is the Coulomb capture radius, e being the electric charge, k the Boltzmann constant, ϵ the dielectric constant of the medium, and T the absolute temperature.

This relation has been obtained under the assumption that the initial distribution of thermalized pairs is an isotropic function. Equation (1) predicts that the escape probability is independent of the field for relatively high field values. For sufficiently high fields, the escape probability increases first linearly and then saturates at the asymptotic value of 1. This behavior originates from the fact that at low fields, in the 3D case, the isotropic motion of the carriers is controlled by diffusion and there is a finite probability of escaping geminate recombination even at vanishing fields.

The situation is expected to be quite different when the motion of the carriers is restricted to one dimension. In this case the probability of escape is, in the absence of fields, zero, as a diffusing carrier will always return to the origin. However, the presence of the field will greatly affect this probability. A 1D Onsager model for the photogeneration of charge carriers in molecular crystals with highly anisotropic, quasi-one-dimensional electronic conduction, has been worked out by Haberkorn and Michel-Beyerle.[23] These authors have considered the case of a one-dimensional random walk of carriers under the influence of an external electric field and an image force. Under the double restriction $a<r_c$ and $E<kT/er_c$, the escape probability for 1D takes the relatively simple form

$$\Phi_{1D}=\frac{ea^2E}{r_ckT}\exp(-r_c/a), \quad a<r_c, \quad E<kT/er_c\ . \quad (2)$$

As we have anticipated, at low fields the escape probability is sensitive to the field, increasing linearly with it. In our measurements, when the direction of the current coincides with the stretching direction, the motion of the carriers can be considered essentially one dimensional and the escape probability is given by Eq. (2). On the other hand, when the current flows perpendicularly to the chains a more isotropic situation is attained and Eq. (1) should be used. The distance a of separation of the hot carriers in polyacetylene after thermalization for the isotropic case was evaluated following the treatment by Knights and Davies[24] for amorphous selenium.

The quantity

$$\Delta E=h\nu-E_g+\frac{e^2}{4\pi\epsilon r} \quad (3)$$

represents the excess kinetic energy of the hot carriers over the local potential. In Eq. (3) E_g is the band-gap energy and r the initial electron-hole pair separation. This energy can be dissipated by electron-phonon scattering at a maximum rate given by $h\nu_p^2$. Assuming diffusive motion during thermalization, the electron-hole separation a at the end of the thermalization process is given by the equation[23]

$$\frac{a^2}{\Delta E}=\frac{D}{h\nu_p^2}\ , \quad (4)$$

where D is the diffusion coefficient which can be evaluated from the mobility μ ($D=kT\mu/e$). Therefore, the parameters involved in the calculations are the mobility μ and the phonon frequency ν_p. Estimated values of the mobility range from 1 to 100 $cm^2/V\,s$ depending on the sample and on the type of measurements with the low values being associated with the "macroscopic" mobility as derived from conductivity measurements of doped samples and the high values with "microscopic" mobility as derived from optical and magnetoresistance measurements. If the thermalization time is short enough so that interchain and interparticle hopping can be neglected, values of $\mu\gg1$ should be used since the motion of the carriers takes place within the chain where it has been created. Values ranging from 15 to 50 Å are obtained for $\mu=5$ to 100 $cm^2/V\,s$ and and $\nu_p=1000\ cm^{-1}$.

By inserting Eq. (4) into Eqs. (1) and (2) the dependence of the escape probability as a function of photon energy, applied field, and temperature can be calculated. Figure 8 shows the calculated dependence of the escape probability as a function of the applied external field in both

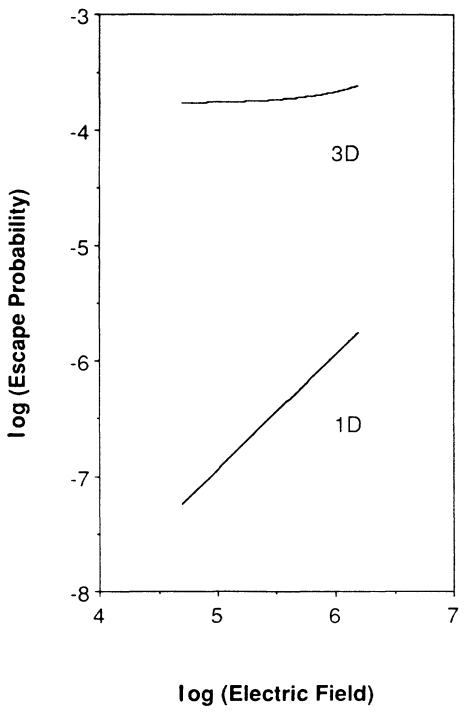

FIG. 8. Log-log plot of the calculated escape probability vs electric field for 1D (||) and 3D (⊥) cases.

1D and 3D cases. Figure 9 shows the dependence of the isotropic escape probability on the photon energy. The curve has to be compared with the measured dependence of the photocurrent on the laser frequency reported in Ref. 14 for an isotropic sample. The agreement is good. Like the experimental photoresponse the escape probability has a nonvanishing value below the gap. At the gap, it exhibits an exponential increase followed by a less steep increase toward the asymptotic value. The behavior above the gap is readily accounted for by considering that photons with increasing energy produce carriers with increasing kinetic energy, which therefore thermalize at a greater distance, with less probability of being recaptured.

The experimental value of the activation energy calculated from the temperature dependence of the cw photoconductivity (Figs. 6 and 7) was about 0.15 eV. This value is in good agreement with previously reported measurements. Kivelson[25] has suggested that the 0.15–0.2 eV is the activation energy for electrons to hop from charged to neutral solitons. This mechanism predicts 3D conduction at low soliton concentration in unoriented samples. The hopping mechanism is consistent with more recent ac conductivity measurements with lightly doped polyacetylene unoriented samples.[26,27] We have calculated the activation energy which controls the temperature dependence of the escape probability. Assuming a photon wavelength $\lambda=500$ nm, an activation energy $E_A \approx 0.1$ to 0.2 eV for $a \approx 15$ to 30 Å is calculated, which agrees well with experimental values for the photocurrent. This good agreement could be indicative of the fact that the temperature dependence of the photocurrent is controlled essentially by the initial recombination of the carriers rather than by their mobility.

Once the escape probability is known the photocurrent intensity can be calculated. Neglecting impurity effects, at low intensity the photocurrent is given by[28]

$$i_{\rm ph}=ed\tau\eta\Phi I[1-\exp(-\alpha t)]\,|\,E\,|\ , \tag{5}$$

where the escape probability Φ is given by Eqs. (1) (3D case) or (2) (1D case), d is the electrode width, e the electron charge, I the laser intensity in photons per second per unit area, μ is the carrier mobility, α is the absorption coefficient, t is the sample thickness, E the applied electric field, and τ the linear recombination lifetime of the carriers. At high intensity, bimolecular (nonlinear) carrier recombination should be expected and the photocurrent intensity is given by[24]

$$i_{\rm ph}=2ed\left[\frac{\eta\Phi I}{\alpha\gamma}\right]^{1/2}\mu[1-\exp(-\alpha t/2)]\,|\,E\,|\ , \tag{6}$$

where γ is the quadratic bimolecular coefficient. Both Eqs. (5) and (6) predict a linear dependence of the photocurrent versus the electric field if the escape probability Φ is independent of the field (3D case) and a superlinear dependence of the current for the 1D case. This is illustrated in Fig. 10, where the photocurrent was calculated using Eq. (6). Experimentally, these two cases correspond to an Ohmic behavior of the photocurrent when the electric field is perpendicular to the stretching direction (3D) and a superlinear dependence when the electric field is parallel to the stretching direction (1D) as observed in our experimental results displayed in Figs. 1 and 2.

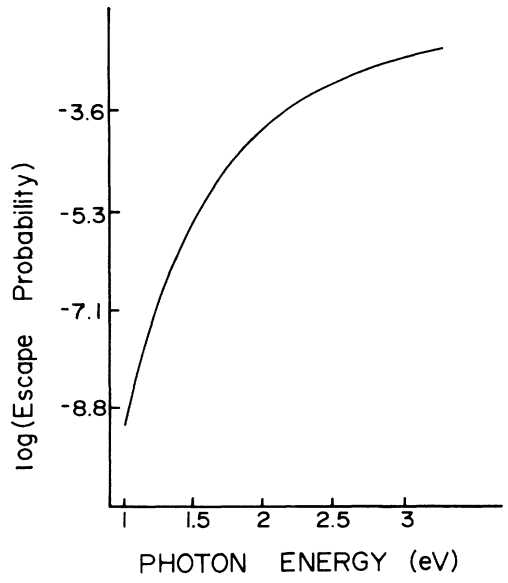

FIG. 9. Calculated dependence of the isotropic escape probability on photon energy for 3D (⊥).

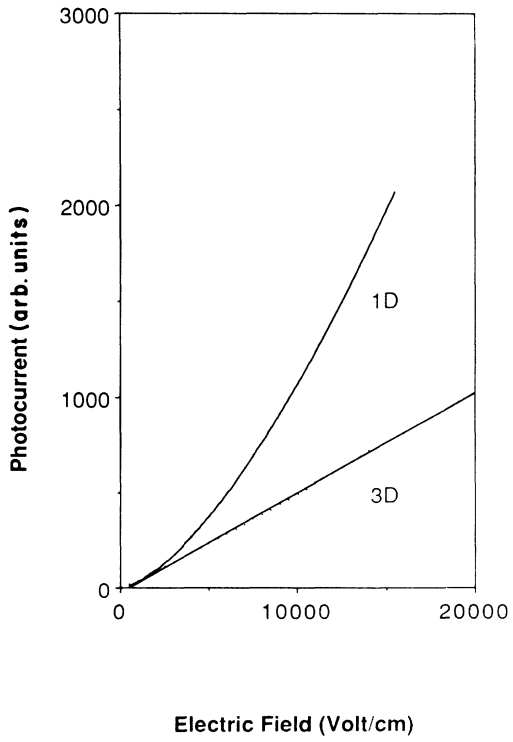

FIG. 10. Calculated photocurrent vs electric field for 1D (||) and 3D (⊥) cases.

According to Eqs. (5) and (6) the 1D photocurrent $i_{ph} \propto E^s$ where $s=2$ in the linear carrier recombination regime and $s=1.5$ in the bimolecular nonlinear regime. Figure 11 shows the photocurrent as a function of incident laser excitation. A changeover from a linear dependence on laser excitation to a sublinear dependence, evidence of bimolecular recombination, is observed around 4 mW. The changeover is reflected in the slope of the *I-V* characteristics shown in Fig. 12, where a log-log plot of the photocurrent as a function of the electric field is given for two different excitations 4 and 10 mW. For values $E \leq 20\,000$ V/cm, at the lower 4 mW excitation the slope is larger ($s \approx 1.7$) than at 10 mW ($s \approx 1.55$), as predicted by Eqs. (5) and (6). For higher field values, as expected the escape probability becomes nonlinear with the field $\Phi \propto E^2$, and the slope becomes $\gg 2$. Figure 13 shows the slope of the 1D characteristic as a function of laser excitation for $E \leq 20\,000$ V/cm. The change from a linear recombination regime ($s \approx 1.9$) to a nonlinear bimolecular regime ($s \approx 1.6$) is clearly demonstrated in good agreement with Eqs. (5) and (6) and the photocurrent dependence on laser excitation. On the other hand, both Eqs. (5) and (6) predict a linear dependence of the photocurrent with the field in the 3D case. This is consistent with our observations. In the 3D case the *I-V* characteristics were always linear or slightly superlinear (a slope ≈ 1.1 for large fields) at all laser excitations and wavelengths.

An obvious limitation of this interpretation is that the 1D and 3D cases are never perfectly realized in *trans*-polyacetylene. Deviations from the pure 1D behavior arise from the presence of defects and chain terminations

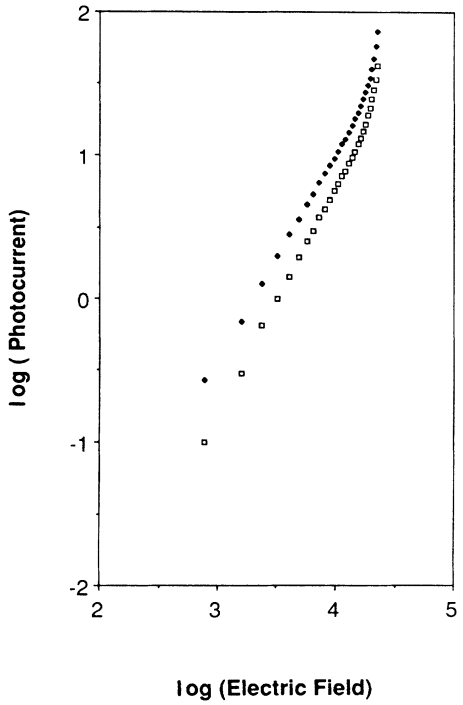

FIG. 12. Log-log plot of the photocurrent vs electric field for 4 (□) and 10 mW (♦) power excitation ($\lambda = 514$ nm).

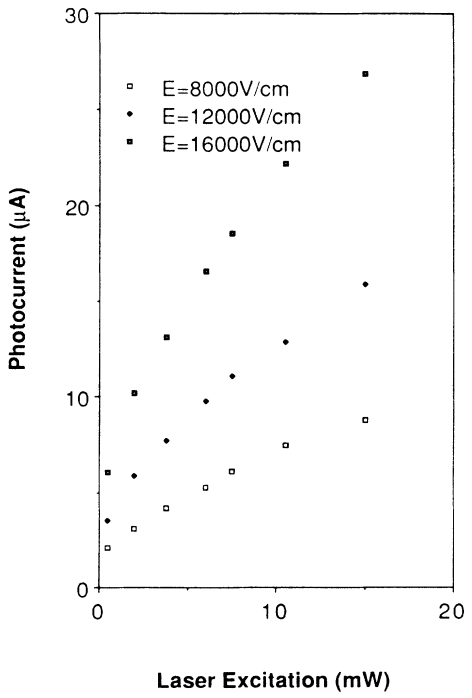

FIG. 11. Photocurrent dependence on laser ($\lambda = 514$ nm) excitation for $E = 8000$ (⊡), 12 000 (♦), and 16 000 V/cm (□).

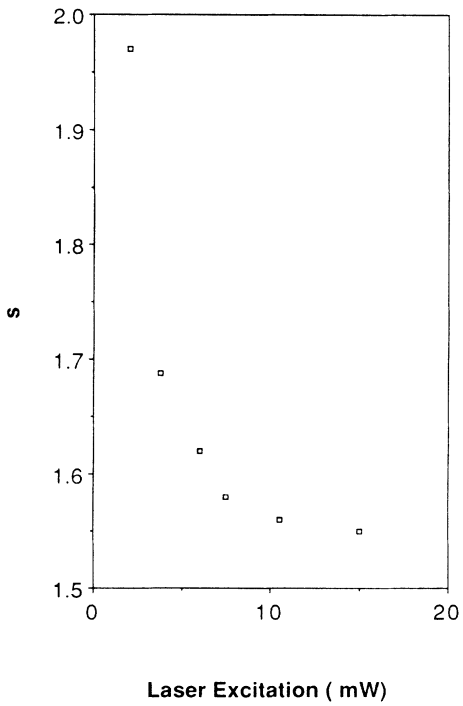

FIG. 13. Slope of the log-log plot of the photocurrent vs electric field as a function of laser excitation ($\lambda = 514$ nm).

and/or to the presence of interchain interaction due to nonvanishing values of the overlap integrals. Wilson[29] has given the expression for the 1D escape probability in the presence of defects which can act as traps for the carriers:

$$\Phi_{1D}=\left[a/w+e\frac{Ea}{kT}+O(E^2)\right]a/r_c\exp(-r_c/a)\ ,$$
$$a<r_c,\quad E<kT/er_c\ , \qquad (7)$$

where w is the distance between traps along the chain. This equation indicates that even at zero field Φ_{1D} is finite and given by

$$\Phi_{1D}=\Phi_{3D}\frac{a^2}{wr_c}\ . \qquad (8)$$

The purely 3D case is also not realized even when the field is applied perpendicularly to the chains. For these reasons, stretched *trans*-polyacetylene films which consist of an assembly of 1D chains organized in a 3D network should exhibit a mixed type of dimensionality in which the parallel photocurrent should exhibit a quasi-1D behavior, while the perpendicular photocurrent should exhibit a quasi-isotropic behavior. The presence of defects, which disrupt the conjugation path thus reducing the 1D character of the charge transfer even for fields parallel to the chains, can be detected from the anisotropy of dark current measurements.

Our measurements give

$$\frac{i_\parallel}{i_\perp}=\frac{\mu_\parallel}{\mu_\perp}=25\ .$$

This value is considerably lower than the calculated anisotropy of the overlap integrals ($S_\parallel=0.23$, $S_\perp=0.0027$ for first intrachain and interchain neighbors, respectively). This suggests that chain terminations, cross links, and other chemical defects localize the carriers, reducing their mobility along the chain, while increasing the interchain transport as they act as hopping sites. From the mobility anisotropy the escape probability anisotropy is estimated through the relation

$$\frac{i_{ph\parallel}}{i_{ph\perp}}=\frac{\sqrt{\phi_\parallel}}{\sqrt{\phi_\perp}}\frac{\mu_\parallel}{\mu_\perp}\ .$$

For $E=2000$ V/cm, $I=25$ mW/cm^2, and $\lambda=500$ nm, our data yield $\phi_\perp/\phi_\parallel=16$, which according to Eq. (8) corresponds to an average distance between defects along the chain of $w=50$ Å for a thermalization distance of 20 Å. These values are only indicative but are in good agreement with the average conjugation length calculated from Raman scattering measurements.

The presence of impurities explains the slightly superlinear ($s\approx1.1$) behavior of the 3D case at relatively high fields (Figs. 1 and 2). The full picture is probably quite complex with a mixture of 3D and 1D terms, where 1D terms dominate for transport along the stretch direction and 3D terms dominate for transport perpendicular to the stretch direction. It is interesting to notice in this respect that the non-Ohmic behavior, which should be characteristic of the quasi-1D case current flow, is no loner observed in samples which were exposed to air for several hours, where a reduction in the conductivity anisotropy is also detected. As noted earlier, the one-dimensional character of the charge transport is reduced in such samples by the addition of oxygen to the double bonds.

CONCLUSION

The main experimental features of the photocurrent as a function of the electric field in highly stretched polyacetylene films are well accounted for by the germinate recombination model. An accurate quantitative evaluation of the experimental data is difficult because of the uncertainty in the values of the mobility and the phonon frequency.

ACKNOWLEDGMENTS

We would like to thank Dr. U. Pedretti for preparing the stretched *trans*-polyacetylene samples. This research is supported in part by the U.S. Air Force Office of Scientific Research under Grant No. 88-0039 and by the Professional Staff Congress of The City University of New York.

[1]T. Ito, H. Shirakawa, and S. Ikeda, J. Polym. Sci. Polym. Chem. Ed. **12**, 11 (1974).
[2]D. White and D. C. Bott, Polym. Commun. **24**, 805 (1983).
[3]G. Lugli, U. Pedretti, and G. Perego, J. Polym. Sci. Polym. Lett. Ed. **23**, 129 (1985).
[4]P. Piaggio, G. Dellepiane, R. Tubino, L. Piseri, and G. Lugli, Solid State Commun. **49**, 895 (1984).
[5]P. Piaggio, G. Dellepiane, L. Piseri, R. Tubino, and C. Taliani, Solid State Commun. **50**, 947 (1984).
[6]G. Masetti, E. Campani, G. Gorini, L. Piseri, R. Tubino, P. Piaggio, and G. Dellepiane, Solid State Commun. **55**, 737 (1985); Chem. Phys. **108**, 141 (1986).
[7]G. Leising, E. Faulques, and S. Lefrant, Synth. Metals **11**, 123 (1985).
[8]T. Tani, P. H. Grant, W. D. Gill, G. B. Street, and T. C. Clark, Solid State Commun. **33**, 499 (1980).
[9]S. Etemad, T. Mitani, M. Ozaki, T. C. Chung, A. J. Heeger, and A. G. MacDiarmid, Solid State Commun. **40**, 741 (1981).
[10]B. R. Weinberger, Phys. Rev. Lett. **50**, 1693 (1983).
[11]B. R. Weinberger, Phys. Rev. Lett. **33**, 86 (1984).
[12]H. Kiess, R. Keller, D. Baeriswyl, and G. Harbeke, Solid State Commun. **44**, 1443 (1982).
[13]Y. Yakoby, S. Roth, K. Menke, F. Keilmann, and J. Kuhl, Solid State Commun. **47**, 869 (1983).
[14]M. Sinclair, D. Moses, and A. J. Heeger, Solid State Commun. **59**, 343 (1986).
[15]R. Dorsinville, S. Krimchansky, R. R. Alfano, J. L. Birman, R. Tubino, and G. Dellepiane, Solid State Commun. **56**, 857 (1985).
[16]H. Bleier, G. Leising, and S. Roth, Synth. Metals Synth. Met.

17, 521 (1987).
[17]A. S. Siddiqui, J. Phys. C **17**, 683 (1984).
[18]R. Dorsinville, R. Tubino, J. L. Birman, and R. R. Alfano, Synth. Met. **17**, 509 (1987).
[19]James C. W. Chien, *Polyacetylene, Chemistry, Physics, and Material Science* (Academic, New York, 1984).
[20]W. P. Su, J. R. Schrieffer, and A. J. Heeger, Phys. Rev. Lett. **42**, 1968 (1979).
[21]J. Orenstein, Z. Vardeny, G. L. Baker, G. Eagle, and S. Etemad, Phys. Rev. B **30**, 786 (1984).
[22]L. Onsager, J. Chem. Phys. **2**, 599 (1934); Phys. Rev. **54**, 554 (1938).
[23]R. Haberkorn and M. E. Michel-Beeyerle, Chem. Phys. Lett. **23**, 128 (1973).
[24]J. C. Knight and E. A. Davies, J. Phys. Chem. Solids **35**, 543 (1974).
[25]S. Kivelson, Phys. Rev. B **25**, 3798 (1982).
[26]D. Emin, K. L. Ngai, J. Phys. (Paris) **44**, 471 (1983).
[27]A. J. Epstein, in *Handbook of Conducting Polymers,* edited by T. A. Skotheim (Dekker, New York, 1986), Vol. 2, p. 1041.
[28]A. S. Siddiqui, J. Phys. C **13**, 2147 (1980).
[29]E. G. Wilson, J. Phys. C **13**, 2885 (1980).